The Effect of Trimethylol Propane Tetraacrylate (TMPTA) and Organoclay Loading on the Properties of Electron Beam Irradiated Ethylene Vinyl Acetate (EVA)/Natural Rubber (SMR L)/Organoclay Nanocomposites

Hanafi Ismail,[1] Yamuna Munusamy,[1] M. Mariatti,[1] Chantara Thevy Ratnam[2]

[1]*Polymer Division, School of Materials and Mineral Resources Engineering, Universitii Sains Malaysia, Nibong Tebal, Penang 14300, Malaysia*
[2]*Radiation Processing Technology Division, Malaysian Nuclear Agency, Bangi, Kajang, Selangor 43000, DE, Malaysia*

Received 17 October 2008; accepted 15 August 2009
DOI 10.1002/app.31415
Published online 26 March 2010 in Wiley InterScience (www.interscience.wiley.com).

ABSTRACT: Ethylene vinyl acetate (EVA)/natural rubber (SMR L)/organoclay nanocomposites were prepared by melt blending technique with 0–10 phr organoclay loading and 3 phr TMPTA. Electron beam initiated crosslinking on these samples was carried out using a 3.0 MeV electron beam machine with doses ranging from 50 to 200 kGy. XRD results proved that dispersion of organoclay in the nanocomposites was slightly improved by irradiation with TMPTA. This was further supported by transmission electron microscopy images, where the nanoscale dispersion of organoclay was more homogenous throughout the irradiated polymer matrix compared to nonirradiated samples. TMPTA also increased the gel fraction yield, tensile properties and thermal stability of the irradiated neat EVA/SMR L and its nanocomposites. TMPTA was found to act as a crosslink initiator, which promotes crosslink bridges via free radical mechanism in EVA/SMR L matrix. SEM observation shows that the fracture behavior of the irradiated neat EVA/SMR L and its nanocomposites with TMPTA is significantly different compared to the fracture behavior of the nonirradiated neat EVA/SMR L. The distinct failure surface structure formed in the irradiated samples with TMPTA explains the overall higher value of tensile properties. © 2010 Wiley Periodicals, Inc. J Appl Polym Sci 117: 865–874, 2010

Key words: TMPTA; electron beam irradiation; nanocomposites; Organoclay; tensile properties; thermal stability

INTRODUCTION

Blends of natural rubber (NR) and ethylene vinyl acetate (EVA) are potential to be used as a zero halogen material in cable industry to replace PVC.[1,2] However a large amount of inorganic fillers such as aluminum trihydroxide or magnesium hydroxide is needed to reach the same flame retardant properties as PVC.[3] Incorporation of these fillers at high loadings causes detrimental effects to the mechanical properties of composites. Recent research developments shows that incorporation of nanofillers such as montmorillonite (MMT) at low loading (<10 wt %) can improve the flame retardancy and thermal stability of various polymer blends without causing negative effects to the strength of the materials.[4,5]

Electron beam irradiation can be utilized to crosslink both the EVA and NR to further improve the mechanical properties and thermal stability of the blend.[6,7] Furthermore now the manufacture of large quantities of wire and cables insulations is based on irradiation crosslinking.[8,9] To produce a low cost electron beam irradiated blends, crosslink initiators can be used. Studies showed that a small amount of crosslink initiators can induce crosslinking at lower irradiation dosage[10] and reduce degradation during the process.[11]

Free radicals are formed in polymers by heating peroxide or exposure to UV light and irradiation. These free radicals then extract hydrogen from polymer chains and polymer radicals were formed. These polymer radicals then react with other polymer radicals to form carbon–carbon crosslinks. The crosslink initiators will provide more reactive sites where this reaction can occur. Crosslink initiators are classified into two types based on their contribution to cure. Type I crosslink initiators increase both rate and state of cure. It is typically polar, multifunctional low molecular weight compounds which form very reactive radicals through addition reactions.

Correspondence to: H. Ismail (hanafi@eng.usm.my).
Contract grant sponsor: Universiti Sains Malaysia; contract grant number: 6035216.

These monomers can be homopolymerized or grafted to polymer chains. Type II crosslink initiators form less reactive radicals and only contribute to state of cure. They form radicals through hydrogen abstraction.[12]

In this article, TMPTA was selected as a crosslink initiator for organoclay filled EVA/ SMR L nanocomposites. TMPTA is a multifunctional vinyl monomer which is highly reactive towards free radicals. It is Type I crosslink initiator. The effect of TMPTA on the tensile properties, morphology, gel fraction and thermal stability of the nanocomposites were investigated.

EXPERIMENTAL

Materials

The EVA with 15% vinyl acetate content was supplied by The Polyolefin Company (Singapore) Pte. (Cosmothene Eva H2020). The NR used was Standard Malaysian Rubber (SMR L) with Mooney viscosity of ML (1+ 4) = 140. SMR L was purchased from Kumpulan Guthrie Sdn. Bhd, Seremban, Malaysia. Organoclay was supplied by Nanocor (USA) (Nanomer 1.30T). Nanomer 1.30T was surface modified MMT with 15–30 wt % octadecylamine. The organoclay is in powder form with 18–23 μm mean dry particle size. Trimethylolpropane triacrylate (TMPTA) is a product of UCB Asia Pacific, Malaysia.

Preparation of nanocomposites

Before blending organoclay was vacuum dried at 80°C for 24 hours.[13] The EVA/ SMR L nanocomposites were prepared by melt mixing in a Haake Rheomix Polydrive R 600/610 at 120°C and rotor speed of 50 rpm. The blend ratio of SMR L and EVA was fixed at 50 : 50 and the organoclay loading was varied from 0 to 10 phr. To study the effect of crosslink initiator, samples with 3 phr TMPTA was prepared. EVA, organoclay and TMPTA was premixed in a beaker at room temperature for 5 min. The mixture was charged into the mixing chamber and allowed to mix for 3 min. Then SMR L was discharged into the mixing chamber and the mixing was continued for another 3 min. The nanocomposites were compression molded in an electrically heated hydraulic press, KAO compression molding machine. Hot press procedures involved preheating at 120°C for 3 min, followed by compressing for 2 min at the same temperature. Then the samples were cooled for 2 min to produce sheet with 1 mm thickness.

Irradiation

The molded sheets were irradiated using a 3 MeV electron beam accelerator NHV EPS-3000 at a dose range of 0–200 kGy. The acceleration energy, beam current, and dose rate were 2 MeV, 2 mA, and 50 kGy per pass, respectively.

X-ray diffraction analysis (XRD)

XRD spectra were recorded with Siemens D5000 diffractometer in step scan mode using Ni-filtered Cu K_α radiation (0.1542 nm wavelength). Powder samples (i.e. organoclay) were scanned in reflection, whereas the molded composites in transmission mode in the angle interval of $2\Theta = 2$–10° in steps 0.05.

Transmission electron microscopy (TEM)

Transmission electron microscope (100 kV acceleration voltage), Philips CM12 model, was used to study the morphology of the nanocomposites. Ultra thin specimens were used to study the organoclay dispersion inside polymer matrix. The ultra thin specimens were sectioned using cryogenic ultramicrotome Leica-Reichert Supernova, Universiti Putra Malaysia.

Gel fraction

The gel fraction was determined by extraction in xylene at 140°C. The blends were solvent extracted with xylene for 48 h and the extracted samples were dried at constant weight. The gel fraction was calculated according to eq. (1)

$$\text{Gel fraction} = (W/W_0) \times 100 \quad (1)$$

where W and W_0 are the weight of the dried sample after extraction and the weight of the sample before extraction, respectively.

Tensile properties

Tensile test was done in accordance with ASTM D638 on an Instron 3366 tensile testing machine. Crosshead speed of 50 mm/min was used. The samples were prepared according to ASTM D638 Type I specifications. The test specimen thickness was 1 mm and variation did not exceed ±2%. The standard test pieces were cut using a Wallace die cutter. Five samples were used for tensile test and an average of results was taken as the resultant value.

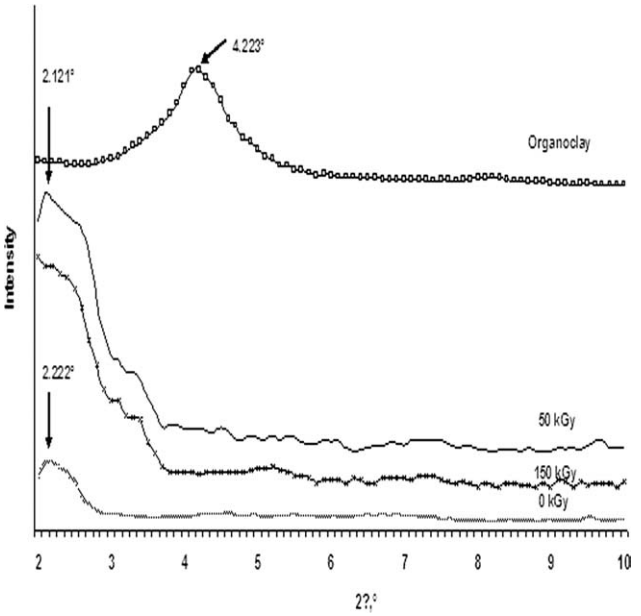

Figure 1 X-ray diffraction pattern for pristine organoclay, irradiated with TMPTA and nonirradiated EVA/SMR L nanocomposites with 2 phr organoclay loading.

Morphology study

The effect of irradiation and organoclay loading on the tensile fracture surface morphology of the nanocomposites were studied using SUPRA36VP-24–58 field emission scanning electron microscopy (FESEM). All samples were examined after sputter coating with gold to avoid electrostatic charging and poor image resolution. The FESEM photographs were taken at a magnification of 2000×.

Thermo gravimetric analysis

Thermal decomposition of the nanocomposites was determined using thermo gravimetric analysis (TGA) with Perkin Elmer Analyzer. Thermograms of ~ 10 mg samples were recorded from 50 to 600°C at a heating rate of 10°C/min under nitrogen flow.

RESULTS AND DISCUSSION

X-ray diffraction analysis

XRD pattern for OMMT and EVA/SMR L/organoclay nanocomposites with 2 and 8 phr organoclay loading are displayed in Figures 1 and 2 respectively. Nanostructure was formed in all the irradiated with TMPTA and nonirradiated nanocomposites. The diffraction peaks for the irradiated nanocomposites were moved to a lower angle compared to nonirradiated samples. Thus the interlayer spacing between the individual silicate layers have been further increased in the irradiated nanocomposites with TMPTA. This might be due to the formation of polar groups, free radicals and ions by electron beam irradiation, which have high mobility and can diffuse in between the silicate layers.[14] This will further enhance the intercalation of polymer chains in organoclay galleries.[15]

The energy from electron beam radiation will knock out one hydrogen atom from polymer chain, thus produce EVA and SMR L macro molecular radicals.[16] In addition alkyl ammonium on the surface of organoclay can undergo Hoffman reaction which will generate ammonium ions, acidic sites in the aluminosilicates and corresponding olefin. The acidic sites can accept single electron from donor molecules with low ionization leading to formation of more free radicals.[17]

EVA/SMR L filled with 8 phr organoclay loading showed a second diffraction peak. The diffraction angle for these peaks was almost the same as that of pristine organoclay, indicating that some organoclay remained as agglomerates.[4]

Transmission electron microscopy

Intercalation, exfoliation and agglomeration of organoclay inside polymer matrix can be observed for both the nonirradiated and irradiated nanocomposites. However the TEM images shows that the intercalation and exfoliation of nanocomposites were further enhanced in the irradiated samples,

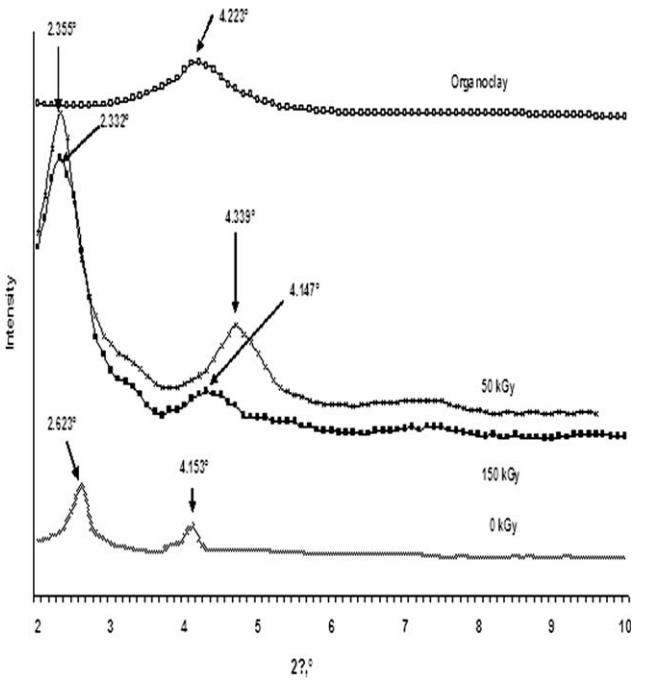

Figure 2 X-ray diffraction pattern for pristine organoclay, irradiated with TMPTA and nonirradiated EVA/SMR L nanocomposites with 8 phr organoclay loading.

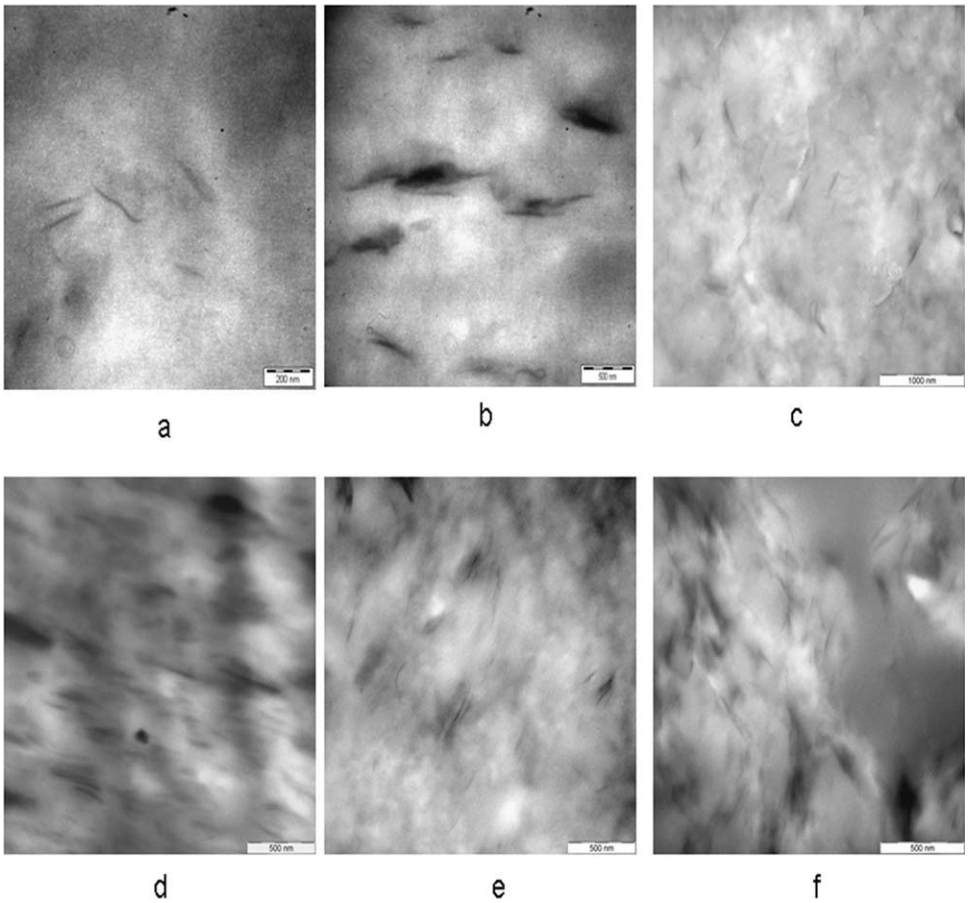

Figure 3 Transmission electron micrograph for nonirradiated EVA/SMR L filled with (a) 2 phr organoclay (b) 8 phr organoclay, 50 kGy irradiated EVA/SMR L filled with (c) 2 phr organoclay (d) 8 phr organoclay and 150 kGy irradiated EVA/SMR L filled with (e) 2 phr organoclay and (f) 8 phr organoclay.

Figure 3(c–f) compared to the nonirradiated ones, Figure 3(a,b). In addition the dispersion of organoclay is also more homogenous throughout the polymer matrix in the irradiated nanocomposites. Agglomerates were observed for nanocomposites with 8 phr organoclay loading for both the nonirradiated and irradiated samples but the numbers of agglomerates have been reduced with irradiation. As explained earlier, highly mobile macro-molecular free radicals and ions were formed during radiation. These radicals and ions can diffuse in between the individual silicate layers and further improve the dispersion of organoclay.

Closer observation on the images of irradiated nanocomposites showed that the dispersed organoclay were oriented in a regular direction compared to the nonirradiated nanocomposites. Similar morphology evolution of organoclay in irradiated polymer nanocomposite was reported by Lu et al. (2002).[18] Natural MMT consists of negatively charged layered silicates.[19] It is noteworthy that organoclay used in this research is modified with 15–30 wt % octadecylamine and therefore some percentages of the organoclay surface still remain negatively charged. The negatively charged surfaces can terminate macromolecular polymer cations and form dangling polymer chains.[20] New polymer-clay interface were formed and may be responsible for the orientation of clay in regular direction.

Gel fraction

Generally the yield of irradiation induced crosslinking can be estimated from gel fraction.[21] Figure 4 shows the gel fraction yields for the irradiated nanocomposites without and with TMPTA respectively. The gel fraction for the neat EVA/SMR L and its nanocomposites increased with increment of irradiation dosage for both the nanocomposites with and without TMPTA. Apparently at all irradiation dosage the gel fraction values for all the nanocomposites are lower than that for the pristine blend. Electron beam irradiation can induce the formation of NR and EVA radicals. These radicals can be scavenged by organoclay, thus the radical–radical interaction hindered and the crosslink network formation

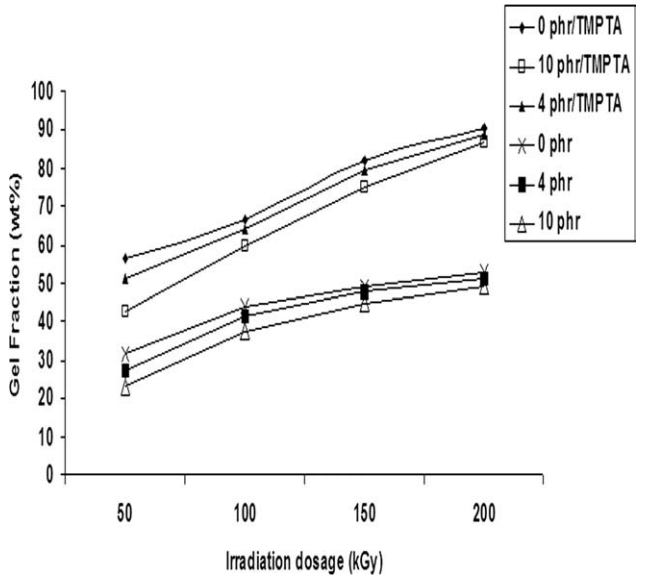

Figure 4 Gel fraction for irradiated neat EVA/SMR L and EVA/SMR L nanocomposites with and without TMPTA.

will be reduced.[22] In addition organoclay nanoparticles also block the sites for crosslinking in the polymeric matrix due to the nano level dispersion of organoclay.[23,24]

However incorporation of TMPTA into the irradiated nanocomposites has improved the gel fraction yield at all irradiation dosage and organoclay loading. The higher values of gel fraction indicate a more efficient formation of three dimensional network structures. TMPTA is a well known reactive additive, which forms crosslink bridges by an irradiation induced free radical mechanism, thus improves the gelation of nanocomposites.

Tensile properties

The tensile strength for all the nanocomposites without and with TMPTA is shown in Figures 5 and 6,

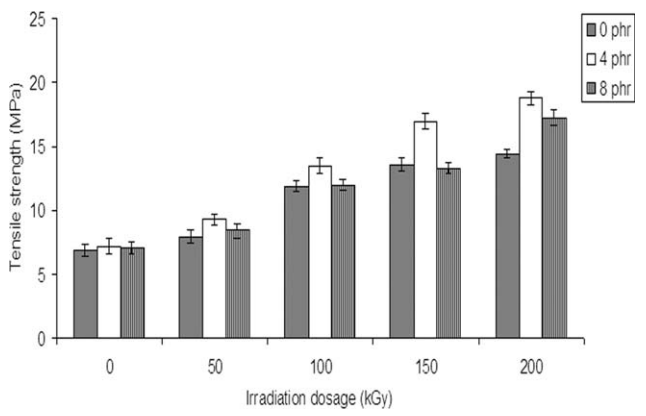

Figure 5 Tensile strength of irradiated neat EVA/SMR L and EVA/SMR L nanocomposites without TMPTA.

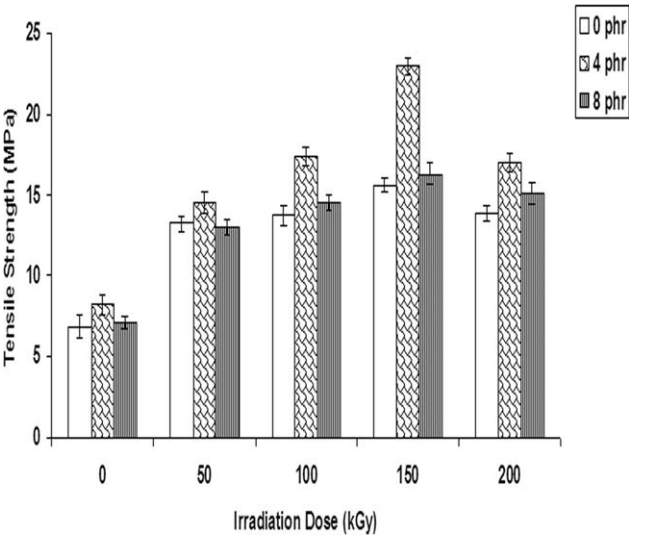

Figure 6 Tensile strength of irradiated neat EVA/SMR L and EVA/SMR L nanocomposites with TMPTA.

respectively. At 50, 100, and 150 kGy the nanocomposites with TMPTA exhibit higher strength compared to nanocomposites without TMPTA. The optimum tensile strength for nanocomposites without TMPTA (18.80 MPa) was achieved at irradiation dosage 200 kGy and organoclay loading 4 phr, whereas, for nanocomposites with TMPTA the optimum tensile strength (22.96 MPa) was achieved at 150 kGy and 4 phr organoclay loading. Moreover the tensile strength for nanocomposites with TMPTA decreased as the irradiation dosage increased up to 200 kGy. Elongation at break was initially increased up to

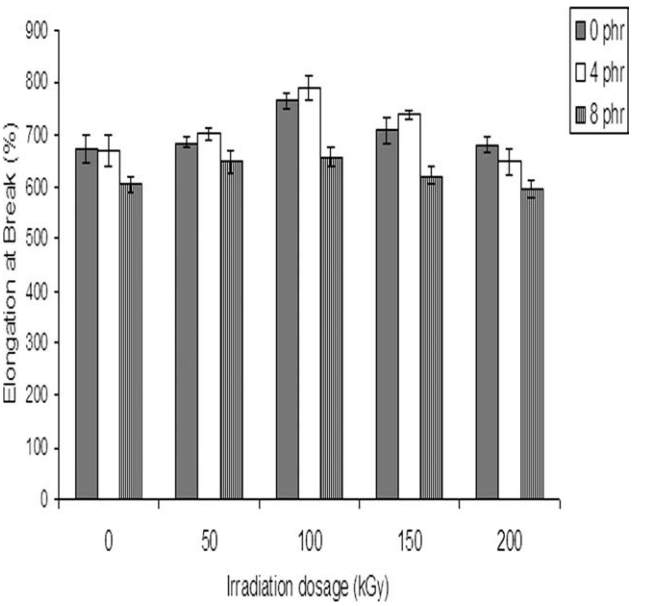

Figure 7 Elongation of break of irradiated neat EVA/SMR L and EVA/SMR L nanocomposites without TMPTA.

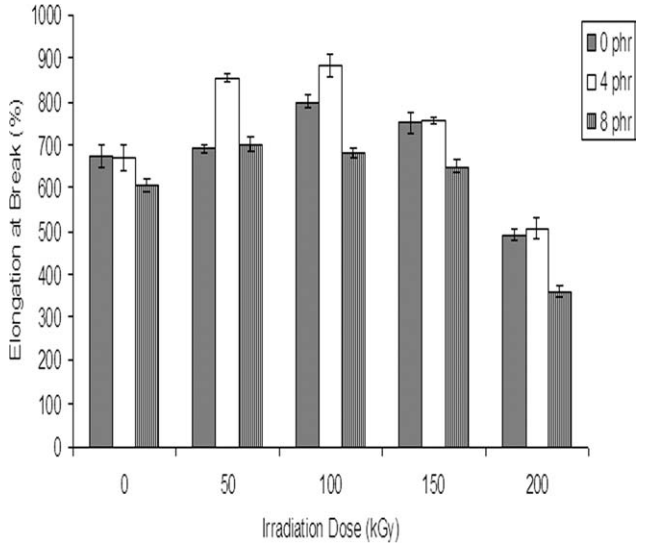

Figure 8 Elongation of break of irradiated neat EVA/SMR L and EVA/SMR L nanocomposites with TMPTA.

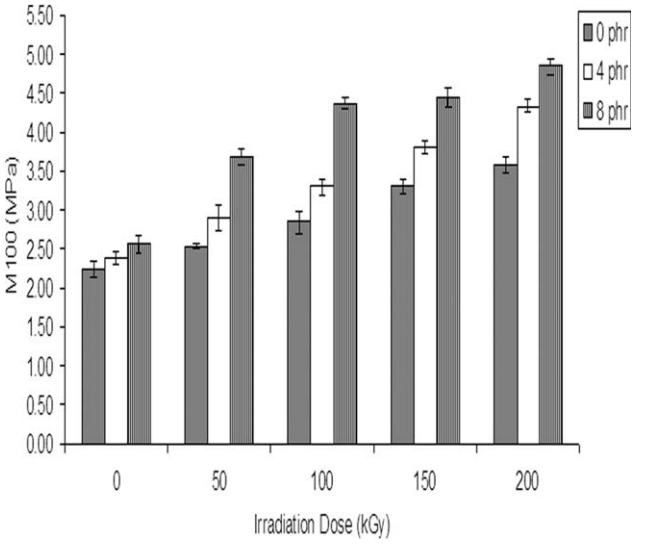

Figure 10 Stress at 100% elongation (M100) of irradiated neat EVA/SMR L and EVA/SMR L nanocomposites with TMPTA.

100 kGy and then decreased with the irradiation dosage for both the nanocomposites without and with TMPTA as shown in Figures 7 and 8, respectively.[25] However the elongation at break reduction at 200 kGy was sharper for nanocomposites with TMPTA.

Tensile strength and elongation at break depend mainly on the degree of crosslinking and strain induced crystallization. In nanocomposites with TMPTA large network structure was formed up to 150 kGy, whereas, at higher irradiation dosage these network structure become smaller because additional crosslinks were formed in between the already crosslinked macromolecule. Therefore at excessive degree of crosslinking the network structure formed were more severe and complex. When strain was subjected to the large network (up to 150 kGy), the chain will extend, tendency for chain slippage will reduce and the degree of chain alignment will increase, therefore strain induce crystallization increase. However when the network was more severe and complex (200 kGy), the degree of chain

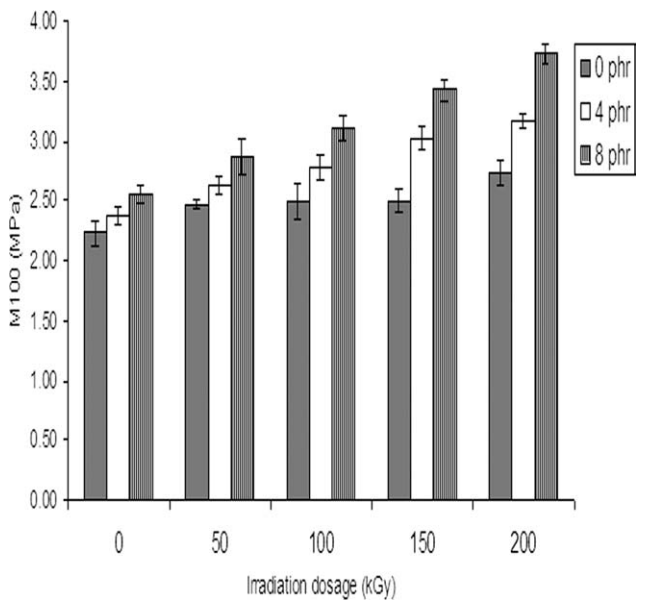

Figure 9 Stress at 100% elongation (M100) of irradiated neat EVA/SMR L and EVA/SMR L nanocomposites without TMPTA.

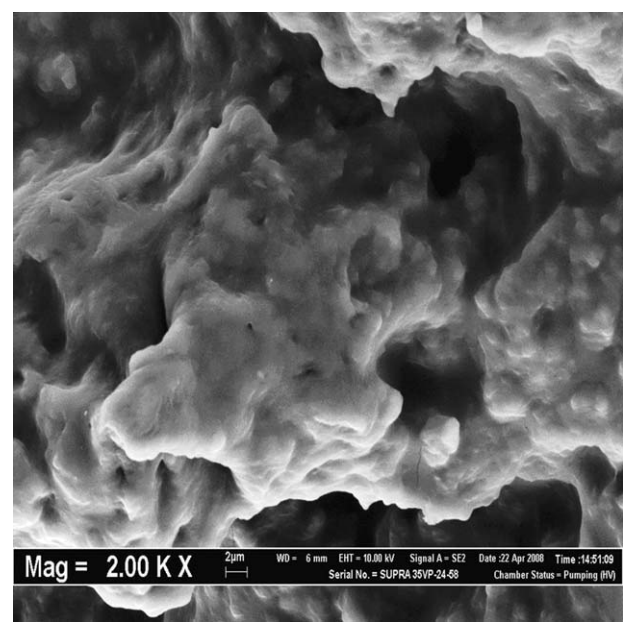

Figure 11 Tensile fracture surface for nonirradiated neat EVA/SMR L.

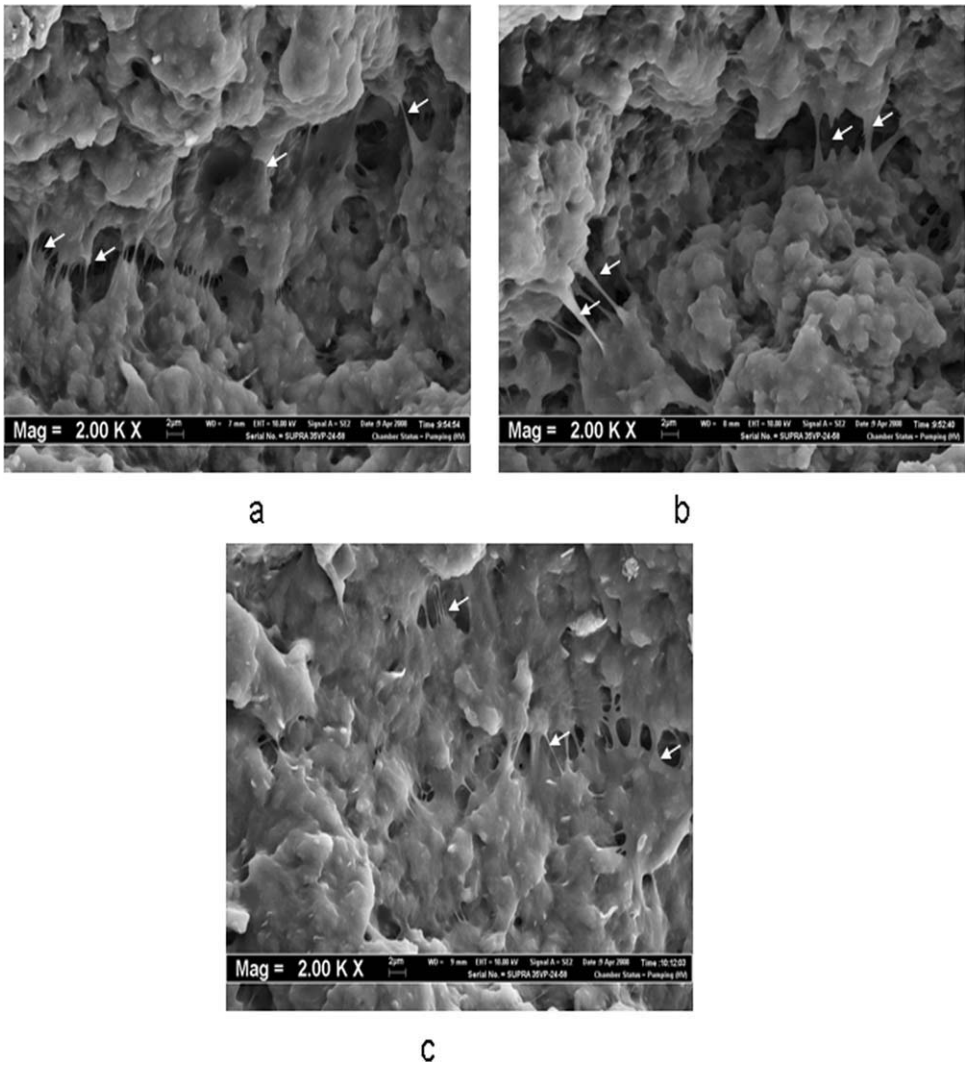

Figure 12 Tensile fracture surface of irradiated (50 kGy) with TMPTA (a) neat EVA/SMR L (b) EVA/SMR L nanocomposites with 4 phr organoclay and (c) EVA/SMR L with 8 phr organoclay.

alignment was lower and therefore strain induced crystallization was lower.[26] The tensile strength of the irradiated nanocomposites without TMPTA increased proportionally to irradiation dosage maybe because the formation of the large network was not enough as indicated by gel fraction results.

For all the irradiated nanocomposites with and without TMPTA, the highest improvement in tensile strength and elongation at break was achieved at 4 phr organoclay loading but both of these properties decrease as the organoclay loading increased to 8 phr loading. Organoclay are well dispersed at low loading, whereas, at high loading agglomerates are formed. These agglomerates can act as stress concentration point which will reduce the tensile strength of nanocomposites.

The stress at 100% elongation (M100), Figures 9 and 10 improved proportionally to the increment of irradiation dosage and organoclay loading. Generally the M100 values for nanocomposites with TMPTA are higher compared to nanocomposites without TMPTA.

The increase in M100 with irradiation dose and organoclay loading can be related to the increased formation of radiation induced crosslinking[27] and demobilizing effect of organoclay on the polymeric chain.[28]

SEM studies

The significant improvements in tensile properties of the irradiated EVA/SMR L samples with incorporation of TMPTA and organoclay were further explained by using the SEM micrographs. The fracture behavior of the non irradiated neat EVA/SMR L blend as shown in Figure 11 is distinct from the fracture behavior of irradiated nanocomposites, Figure 12(a-c) and Figure 13(a-c). Fibrils like structure (as indicated by white arrows) were formed in the irradiated nanocomposites.[29] The stretched and

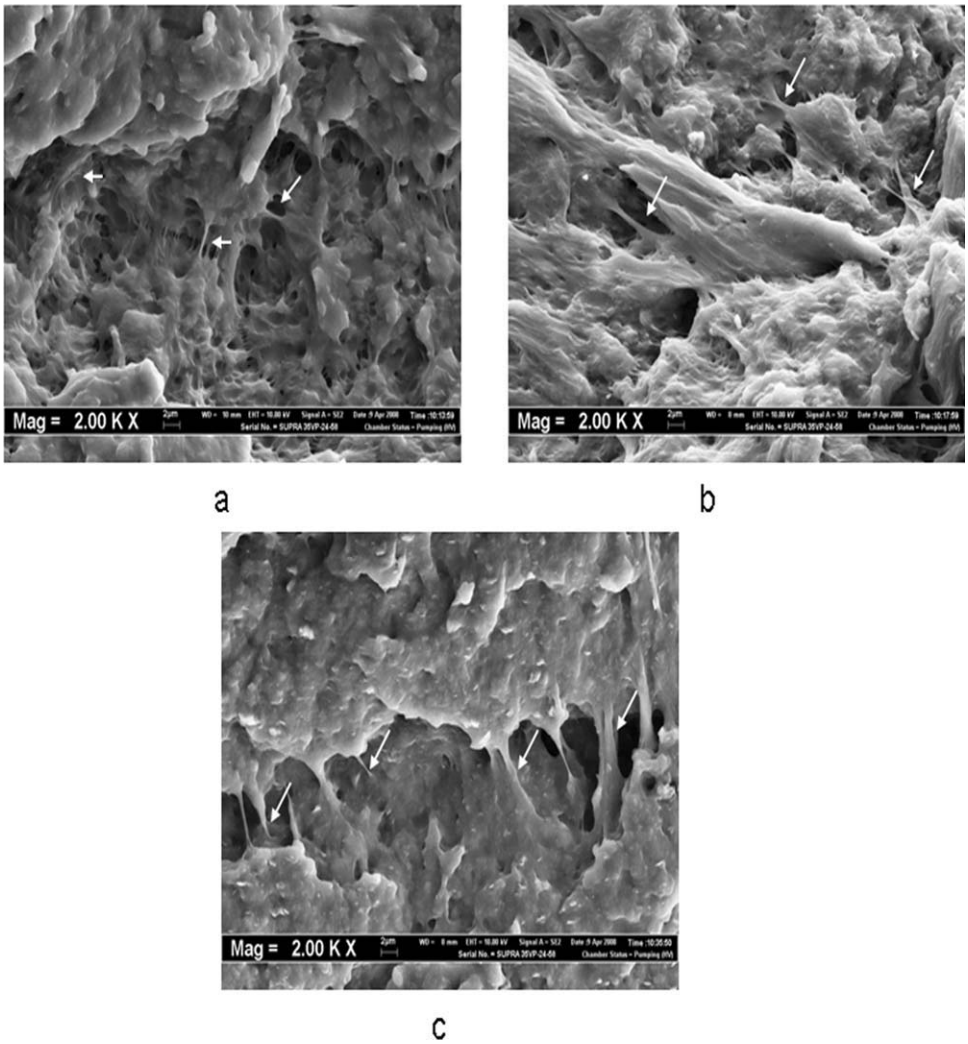

Figure 13 Tensile fracture surface of irradiated (150 kGy) with TMPTA (a) neat EVA/SMR L (b) EVA/SMR L nanocomposites with 4 phr organoclay and (c) EVA/SMR L with 8 phr organoclay.

elongated matrix indicates higher resistance towards failure.

At 150 kGy, Figure 14(a–c) the formation of elongated fibril like structure was more significant. This can be used to explain the higher tensile properties of the nanocomposites at 150 kGy compared to 50 kGy. Furthermore at all irradiation dosage samples with 4 phr organoclay loading, Figures 12(b) and 13(b) shows a ductile fracture surface with more longer and finer fibril like structure, whereas, at 8 phr organoclay loading Figures 11(c) and 12(c) the fibril like structure were shorter and thicker. This indicates that at 4 phr organoclay loading the crosslink matrix can be further deformed and absorb more energy before failure, thus, exhibit a higher strength properties. However when 8 phr organoclay was used, the rigidity of the nanocomposites increased, thus, reduce the ability of the matrix to deform when subjected to strain.[30] In addition the agglomerated organoclay at higher loading acts as stress concentration point which reduce the strength of polymer matrix.

Thermal stability

In this article only one TGA graph is presented, Figure 14. This thermogram represents the typical thermal decomposition behavior for all the neat EVA/SMR L and its nanocomposites. It can be seen that the thermal decomposition of either neat EVA/SMR L or EVA/SMR L nanocomposites passes through two stages upon heating from 50°C to 600°C. The first was attributed to the SMR L phase degradation and acetic acid loss from EVA and the second was due to degradation of the polyethylene backbone in EVA.[31]

The thermal stability of the irradiated nanocomposites with TMPTA has been improved compared with the thermal stability of pristine EVA/SMR L blend. The improvements in thermal stability of the irradiated nanocomposites are due to the formation of more compact three dimensional crosslink networks which is more stable against formation of gaseous degradation product[32] and the barrier effect of

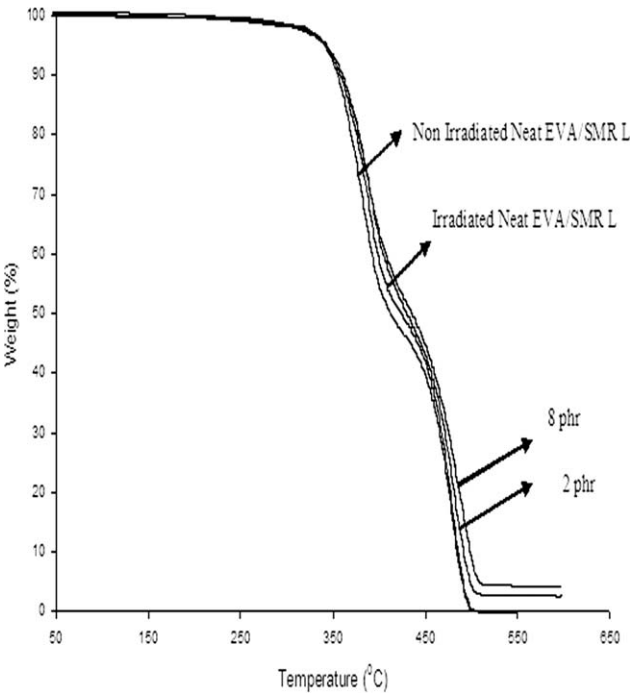

Figure 14 Thermogram for nonirradiated EVA/SMR L, irradiated with TMPTA neat EVA/SMR L and irradiated with TMPTA EVA/SMR L/organoclay nanocomposites at 50 kGy.

organoclay. Well dispersed individual layers of intercalated/exfoliated clay platelets form torturous path which inhibit the passage of volatile degradation product from the polymer matrix.[33] Furthermore many studies proven that organoclay enhances the formation of compact char structure on the surface of polymer matrix. The formation of strong acidic proton sites during thermal decomposition of octadecylamine on the surface of organoclay catalyzes the formation of stable char residue.[34] These char hinders the diffusion of volatile decomposition products from the nanocomposites.[35] Therefore the $T_{onset\ 1}$, $T_{onset\ 2}$, $T_{max\ 1}$, and $T_{max\ 2}$ increased meanwhile the weight loss due to diffusion of volatile degradation product from nanocomposites to atmosphere reduced significantly for nanocomposites irradiated with TMPTA[36] as shown in Tables I and II, respectively.

TABLE I
Thermal Decomposition Temperatures for the Neat EVA/SMR L and its Nanocomposites

Sample	Organoclay loading (phr)	$T_{onset\ 1}$ (°C)	$T_{onset\ 2}$ (°C)	$T_{max\ 1}$ (°C)	$T_{max\ 2}$ (°C)
Nonirradiated neat EVA/SMR L	0	341.09	433.48	377.00	476.00
EVA/SMR L	0	342.86	443.22	383.56	485.00
irradiated	2	343.01	444.85	386.10	487.23
at 50 kGy	8	345.20	449.29	388.25	493.35
EVA/SMR L	0	343.22	445.34	386.73	488.21
irradiated	2	344.33	447.85	388.64	490.78
at 150 kGy	8	346.82	453.91	393.77	494.13

TABLE II
Weight Loss of the Neat EVA/SMR L and its Nanocomposites During Thermal Decomposition

Samples	Organoclay loading (phr)	Weight loss at $T_{max\ 1}$ (%)	Weight loss at $T_{max\ 2}$ (%)
Nonirradiated neat EVA/SMR L	0	10.5114	12.3291
EVA/SMR L	0	9.5443	10.8887
irradiated	2	7.5465	9.4222
at 50 kGy	8	6.1189	7.6790
EVA/SMR L	0	8.5538	8.6672
irradiated	2	6.3337	7.1679
at 150 kGy	8	5.4692	6.6775

CONCLUSION

In the electron beam irradiated neat EVA/SMR L and its nanocomposites, incorporation of TMPTA additive have efficiently initiated the formation of more crosslink bridges in the matrix via free radical mechanism. The gel fraction, tensile properties and thermal stability of the irradiated with TMPTA samples were further improved compared to samples irradiated without TMPTA. At all irradiation dosage the optimum improvement in tensile strength and elongation at break was achieved at 4 phr organoclay loading due to good dispersion of organoclay at low loading, whereas, further increment in the organoclay loading only causes detrimental effects to these properties due to agglomeration of organoclay. The increment in M100 and thermal stability was proportional to the increment of organoclay loading.

References

1. Munusamy, Y.; Ismail, H.; Mariatti, M.; Ratnam, C. T. J Reinf Plast Compos 2008, 27, 1925.
2. Yong, M. K.; Ismail, H.; Ariff, Z. M. Polym Plast Technol Eng 2007, 46, 361.
3. Hull, T. R.; Price, D.; Liu, Y.; Wills, C. L.; Brady, J. Polym Degrad Stab 2003, 82, 365.
4. Tang, T.; Hu, Y.; Wang, S. F.; Gui, Z.; Chen, Z.; Fan, W. C. Polym Degrad Stab 2002, 78, 555.
5. Ismail, H.; Munusamy, Y. J Reinf Plast Compos 2007, 26, 1681.
6. Dahlan, H. M.; Zaman, M. D. K.; Ibrahim, A. Radiat Phys Chem 2002, 64, 429.
7. Mateev, M.; Karageorgiev, M.; Radiat, S. Phys Chem 1998, 51, 205.
8. Ratnam, C. T.; Nasir, M.; Baharin, A. Polym Test 2001, 20, 485.
9. Bhattacharya, A. Prog Polym Sci 2000, 25, 371.
10. Ratnam, C. T.; Zaman, K. Nucl Instrum Methods Phys Res Sect B 1999, 152, 335.

11. Ratnam, C. T.; Nasir, M.; Baharin, A.; Zaman, K. J Appl Polym Sci 2001, 81, 1914.
12. Henning, S. K.; Costin, R. Fundamental of curing elastomer with peroxides coagents. Presented at the Spring 167th Technical Meeting of the Rubber Division, American Chemical Society, Sartomer Company, Inc., USA. May 16–18, 2005.
13. Yang, I.; Tsai, P. Polymer 2006, 47, 5131.
14. Lu, H.; Hu, Y.; Xiao, J.; Kong, Q.; Chen, Z.; Fan, W. Mater Lett 2005, 59, 648.
15. Cerrada, M. L.; Rodriguez-Amor, V.; Perez, V. J Polym Sci Part B: Polym Phys 2007, 45, 1068.
16. Ghazali, Z.; Johnson, A. F.; Dahlan, K. Z. Radiat Phys Chem 1999, 55, 73.
17. Nowicki, A.; Przybytniak, G.; Kornaeka, E.; Mirkowski, K.; Zimek, Z. Radiat Phys Chem 2007, 76, 893.
18. Lu, H.; Yuan, H.; Kong, Q.; Cai, Y.; Chen, Z.; Fan, W. Polym Adv Technol 2004, 15, 601.
19. Zulfiqar, S.; Kausar, A.; Rizwan, M.; Sarwar, M. I. Appl Surf Sci 2008, 255, 2080.
20. Lu, H.; Yuan, H.; Kong, Q.; Cai, Y.; Chen, Z.; Fan, W. Polym Adv Technol 2005, 16, 688.
21. Ratnam, C. T.; Khairul, Z. Polym Degrad Stab 1999, 65, 99.
22. Chattopadhyay, S.; Chaki, T. K.; Bhowmick, A. K. J Appl Polym Sci 2001, 79, 1877.
23. Sharif, J.; Wan Yunus, W. M. Z.; Mohd Dahlan, K. Z. H.; Ahmad, M. H. Polym Test 2005, 24, 211.
24. Alla, S. G. A.; El-Din, H. M. N.; El-Naggar, A. W. N. J Appl Polym Sci 2006, 102, 1129.
25. Basfar, A. A.; Mosnã¡Ček, J.; Shukri, T. M.; Bahattab, M. A.; Noireaux, P.; Courdreuse, A. J Appl Polym Sci 2008, 107, 642.
26. Sharif, J.; Khairul, Z. M. D.; Wan, M. Z. W. Y. Radiat Phys Chem 2007, 76, 1698.
27. Ratnam, C. T.; Zaman, K. Polym Degrad Stab 1999, 65, 481.
28. Stretz, H. A.; Paul, D. R.; Li, R.; Keskkula, H.; Cassidy, P. E. Polymer 2005, 46, 2621.
29. Akinay, A. E.; Tinger, T. J Appl Polym Sci 1998, 67, 1619.
30. Soares, G.; Jansen, P. Polym Degrad Stab 1996, 52, 95.
31. Liu, I.-C.; Tsiang, R. C. C. Nucl Instrum Methods Phys Res Sect B 2002, 197, 228.
32. Wang, Y.; Chen, F. B.; Li, Y. C.; Wu, K. C. Compos Part B 2004, 35, 111.
33. Gilman, J. W. Appl Clay Sci 1999, 15, 31.
34. Bellucci, F.; Camino, G.; Frache, A.; Sarra, A. Polym Degrad Stab 2007, 92, 425.
35. Pandey, J. K.; Reddy, K. R.; Kumar, A. P.; Sing, R. P. Polym Degrad Stab 2005, 88, 234.
36. Zakaria, A.; Badr, Y.; Eisa, W. Polym Compos 2006, 27, 709.